ELSEVIER

www.elsevier.nl/locate/jorganchem

Journal of Organometallic Chemistry 609 (2000) 110–122

Journal of Organometallic Chemistry

The effect of ancillary ligands on intramolecular proton–hydride (NH···HIr) bonding in complexes of iridium(III)

Sung Han Park [a,1], Alan J. Lough [a], Glenn P.A. Yap [b,2], Robert H. Morris [a,*]

[a] *Department of Chemistry, University of Toronto, 80 St. George Street, Toronto, Ont., Canada M5S 3H6*
[b] *Department of Chemistry, University of Windsor, Windsor, Ont., Canada N9B 3P4*

Received 19 February 2000; received in revised form 16 April 2000

Abstract

The reaction of the trihydride $IrH_3(PPh_3)_3$ with HBF_4 in the presence of pyridinethione (SpyH) affords a dihydrido SpyH complex $[IrH_2(\eta^1\text{-SpyH})(PPh_3)_3](BF_4)$ (**1**). Complex **1** undergoes a substitution of one of the PPh_3 ligands by another SpyH to produce $[IrH_2(\eta^1\text{-SpyH})_2(PPh_3)_2](BF_4)$ (**2**). Complex **2** slowly eliminates a dihydrogen molecule to form a known monohydrido complex $[IrH(\eta^1\text{-SpyH})(\eta^2\text{-Spy})(PPh_3)_2](BF_4)$ under mild conditions. $[IrH(CO)(\eta^1\text{-SpyH})_2(PPh_3)_2](BF_4)_2$ (**3**) is obtained from the reaction of known $IrH_3(CO)(PPh_3)_2$ with HBF_4 in the presence of SpyH. The properties of the NH···HIr proton–hydride bonds (also known as dihydrogen bonds) in complexes **1**–**3** are characterized in solution by T_1 NMR measurements and in the solid state by IR measurements and single crystal X-ray diffraction. They are compared with properties of three related complexes to understand the effect of the ancillary ligands on the strength of this non-classical bond. Stronger proton–hydride bonds are formed in complexes with PCy_3 co-donor ligands in comparison with complexes with PPh_3 co-donor ligands. The strength of proton–hydride bonds is decreased in complexes containing more PPh_3 or CO ligands. The best indicators of H···H bond strength are $\Delta\nu$ values from IR and the N···Ir distance from the X-ray structures.

Keywords: Proton–hydride bond; Pyridinethione; SpyH; Trihydride; Dihydrogen; Iridium

1. Introduction

Our group has been investigating the structural types of NH···HIr proton–hydride bonds [1–6] since their existence was recognized by some of us and by Crabtree and co-workers [7–9] in 1994. Related OH···HIr interactions were identified by Stevens et al. [10] and Crabtree and co-workers [7] and labelled 'dihydrogen bonds' [11]. The object of the current study is to prepare triphenylphosphine analogs to the tricyclohexylphosphine complexes already characterized [1,2,4] (e.g. complexes **5** and **6** in Fig. 1). Complexes of the type **5** are obtained by two different routes: (i) a substitution of weakly coordinated solvent molecules [4] in $[IrH_2(solvent)_2(PCy_3)_2]^+$ with pyridinethione (SpyH), the tautomer of 2-mercaptopyridine, or 2-thiazolidinethione or 2-benzothiazolethione; (ii) a reaction of $IrH_5(PCy_3)_2$, with pyridiniumthiol ($HSpyH^+$) [1]. The latter method, when conducted using an excess of hydrogen bond donor ligand and acid, afforded species of the type $[Ir(SpyH\cdots H\cdots HpyS)(SpyH)_2(PCy_3)]^{2+}$ and $[Ir(SpyH\cdots H\cdots HpyS)(\eta^2\text{-Spy})(PCy_3)]^+$ (**6** in Fig. 1) [2].First the route to the known triphenylphosphine complexes of iridium containing proton hydride bonds will be reviewed. The neutral trihydrido aminopyridine ($pyNH_2$) complex $IrH_3(pyNH_2)(PPh_3)_2$ (**I**) [7] was prepared from $IrH_5(PPh_3)_2$ with 2-aminopyridine under very mild conditions (room temperature (r.t.) for several hours) according to Eq. (1). Due to the difficulty in obtaining $IrH_5(PPh_3)_2$ in high yield, a trihydride $IrH_3(PPh_3)_3$ was used in an attempt to make an analogous trihydrido species (**I**, L–NH=SpyH) under similar conditions [3]. The result was the chelation of the pyridinethione ligand to give a complex of type **II** in Eq. (1). As noted in our earlier studies, the protonation of **II** with an acid in the presence of proton donor

* Corresponding author. Tel./fax: +1-416-978-6962.
E-mail address: rmorris@chem.utoronto.ca (R.H. Morris).
[1] Present address: Department of Chemistry, Stanford University, Stanford, CA 94305, USA.
[2] Present address: X-Ray Laboratory, 401 Pavillon d'Iorio, 10 Marie Curie Avenue, University of Ottawa, Ottawa, Ont., Canada.

0022-328X/00/$ - see front matter
PII: S0022-328X(00)00238-2

ligand (SpyH) was attempted to obtain complexes like **5** or **6** but containing PPh_3. However, the reaction produced the monohydrido species **4** (Fig. 1) [3]. Another possible synthetic approach is the use of $IrH_3(PPh_3)_3$ in the direct reaction with HSpy and an acid. This will be described in the first part of this study.

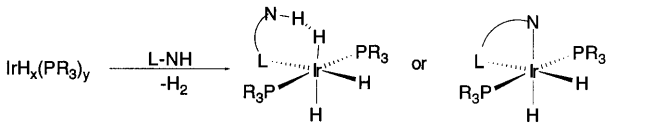

(1)

In the second part of this study, a synthetic approach to hydrido carbonyl complexes containing the SpyH hydrogen bond donor group is described. A carbonyl ligand might be a weaker hydrogen bond acceptor than hydride and may not interfere with the formation of SpyH···HIr bonds. On the other hand, it is a strong π-acid and could influence the strength of the proton hydride bond. Some preliminary results are presented.

Finally, in the last part of this study, the features of the proton hydride bonds in the six pyridinethione complexes described previously or prepared in the current study will be compared to discern factors that influence the strength of this non-classical hydrogen bond.

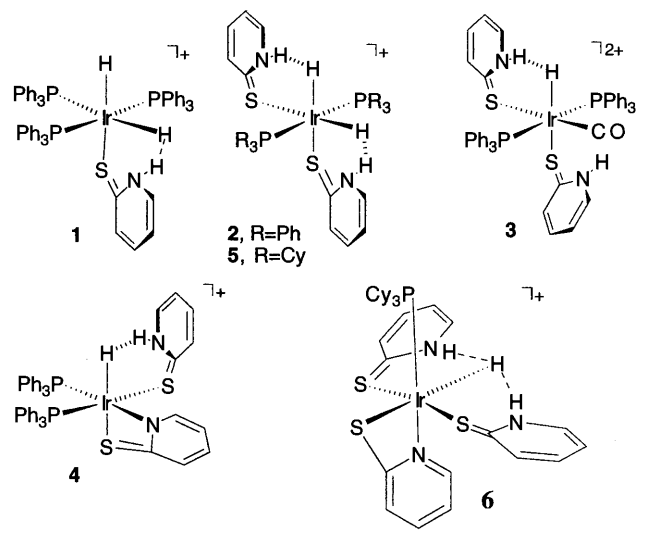

Fig. 1. Iridium(III) complexes possessing one or two proton hydride bonding units.

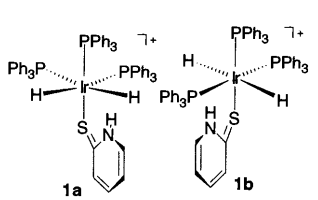

Fig. 2. Possible isomers other than **1** that might form in reaction 2.

2. Results and discussion

2.1. Synthesis of $[IrH_2(\eta^1\text{-SpyH})(PPh_3)_3](BF_4)$ (1)

The reaction of *fac*-$IrH_3(PPh_3)_3$ with tetrafluoroboric acid etherate in the presence of pyridine-2-thione in dichloromethane or chloroform gives a product identified as $[IrH_2(SpyH)(PPh_3)_3](BF_4)$ (**1**) according to Eq. (2). Complex **1** is isolated in 91% yield as a yellow microcrystalline solid which is slightly soluble in $CHCl_3$, toluene, benzene or acetone, but very soluble in CH_2Cl_2. Complex **1** has been also prepared from the mixture of *fac*- and *mer*-isomers of the trihydride which is conveniently obtained in similar yield from iridium trichloride according to a method similar to that of Chatt et al [12].

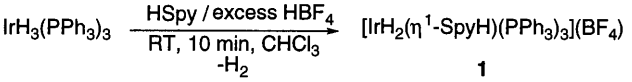

(2)

2.2. Characterization of $[IrH_2(\eta^1\text{-SpyH})(PPh_3)_3](BF_4)$ (1)

Complex **1** has been characterized by microanalysis, NMR techniques (^{31}P- and ^{1}H-NMR, VT–T_1 measurement), infrared spectroscopy, and an X-ray diffraction study. In $CDCl_3$ the $^{31}P\{^1H\}$-NMR spectrum of **1** consists of two signals at 2.23 as a doublet and −0.93 ppm as a triplet with an intensity ratio of 2:1. The appearance of these resonances is monitored by $^{31}P\{^1H\}$-NMR in comparison with the disappearance of the singlet at 10 ppm for the parent trihydride. The pattern of the new resonances indicates the formation of a single isomer with three phosphine ligands in two different magnetic environments. The proton NMR spectrum of **1** in $CDCl_3$ contains assignable peaks for the protons on the pyridine ring, the phenyl groups as well as the hydrides. Peaks for the pyridine ring protons are overlapping with those for the phenyl ring protons in the region from 7.8 to 6.4 ppm. The patterns of the resonances of the two inequivalent hydrides are distinctive at −12.7 and −15.8 ppm. The former appears as a doublet of triplet of doublets due to couplings of *trans* J_{PH} (116 Hz), *cis* J_{PH} (22 Hz), and *cis* J_{HH} (3.6 Hz) while the latter appears as a pseudo quartet of doublets due to couplings with three *cis*-phosphorus nuclei and a *cis*-hydride nucleus. Finally the NH proton resonance appears at 10.9 ppm as a broad singlet.

Other possible isomers such as *fac-cis*-**1a** and *mer-trans*-**1b** depicted in Fig. 2 have not been observed in the product. Probably the former is less favored be-

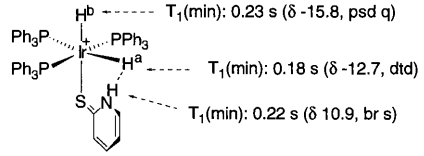

Fig. 3. Comparison of the hydride and NH resonances and their T_{1min} for **1**.

cause of steric congestion caused by the three large phosphine ligands and the latter, because of the instability of *trans*-hydrides. After ca. four weeks, **1** undergoes a partial isomerization in the solid state under laboratory fluorescent light conditions. The isomerization yield is about 10% as judged by the intensity ratio in the proton and phosphorus NMR spectra. The isomerization product is proposed to be the *trans*-hydride **1b** based on the following NMR characterization in CD_2Cl_2. The $^{31}P\{^1H\}$-NMR spectrum of the isomerization product exhibits resonances characteristic of a typical *mer*-phosphine complex as a doublet ($J = 15.67$ Hz) and a triplet ($J = 15.55$ Hz) at -10.05 and -17.32 ppm, respectively. Complex **1a** would also give this pattern. The proton NMR spectrum contains a hydride resonance at -19.75 ppm as a doublet of triplets with coupling constants of 22.4 and 8.85 Hz due to coupling to the phosphorus nuclei in two different *cis*-environments. Two mutually *trans*-hydrides are magnetically equivalent with respect to these three *cis*-phosphorus ligands and a *cis*-pyridinethione ligand. The NH resonance of the monodentate SpyH ligand appears at 12.5 ppm as a broad singlet with half the intensity of the hydride resonances. The fact that the spectrum lacks a resonance with a large *trans*-PH coupling suggests that the *fac*-isomer **1a** is not formed. The intensity of the hydride and NH proton resonances of **1b** relative to those of **1** is about 10% after a month and no further change is observed.

The solid state IR spectrum of **1** contains characteristic bands corresponding to ν(Ir–H) and ν(NH). Bands for ν(Ir–H) at 2063 and 2197 cm^{-1} (KBr) are comparable to those (2214; 2137, 2120 cm^{-1}) for the proton–hydride-bonded complexes $[IrH(\eta^1\text{-SpyH})(\eta^2\text{-Spy})(PPh_3)_2](BF_4)$ **4**, and $[IrH_2(\eta^1\text{-SpyH})_2(PCy_3)_2](BF_4)$ **5**, respectively [1,5]. The ν(NH) of coordinated SpyH in **1** appears as a broad band at 3225 cm^{-1}. This band is similar to that (3236 cm^{-1}) of **4**, but at higher wavenumbers than that (3111 cm^{-1}) of **5**. This probably indicates that the Ir–H···H–N interactions are weaker in **1** and **4** than those in **5**.

The minimum T_1 (T_{1min}) values for the two hydrides and the NH proton of **1** have been obtained at 233 K at 400 MHz. These are shown in Fig. 3 with a proposed structure of **1**, the one found by X-ray diffraction (see below). The T_1 minima are 0.18 and 0.23 s for the hydrides and 0.22 s for the NH proton in CD_2Cl_2. The shorter T_{1min} of 0.18 s is assigned to the resonance for the hydride (H^a) *cis* to the SpyH ligand. The relaxation rate (5.6 s^{-1}) for this T_1 value is attributed to two PPh_3 protons (1.0 s^{-1}, 2.4 Å), *cis*-hydride (H^b) (0.7 s^{-1}, 2.3 Å) and the NH proton (3.9 s^{-1}). The calculation [13] gives the $H^a\cdots H(N)$ distance of ca. 1.71 Å from the T_{1min} of the hydride (H^a). Using a T_{1min} of 0.22 s for the NH proton and the sole relaxation rate contribution (3.2 s^{-1}) from the hydride, after subtraction of a contribution of 1.4 s^{-1} for ^{14}N at 1.0 Å, the H···H distance of ca. 1.77 Å is obtained.

H/D exchange experiments have been carried out at r.t. with D_2 gas or CH_3OD. Exposure of a CD_2Cl_2 solution of **1** to D_2 gas at 1 atm for 3 min resulted in no significant changes in the intensities of the NH and IrH resonances in the proton NMR spectrum. This contrasts with the reactivity of **5** where extensive exchange of ND for NH and IrD for IrH was observed under comparable conditions [1]. Isotopic shifts are observed when this solution is treated with an excess of CH_3OD, a result of the deuteration at the NH group. After 15 h in the presence of CH_3OD the pseudoquartet resonance at -15.7 ppm for the hydride *trans* to the SpyH ligand becomes a superimposed multiplet (15 lines evenly spaced) centered at -15.48 ppm while the doublet of triplet of doublet resonance at -12.7 ppm for the other hydride is broadened by unresolved resonances due to isotopomers. Similarly, in the $^{31}P\{^1H\}$-NMR spectrum, the resonance at -0.66 ppm (triplet) for the phosphine ligand *trans* to the hydride is unchanged while that of the other two equivalent phosphorus nuclei has shifted ($\Delta\delta = 0.079$) from 1.72 (doublet) to 1.82 ppm (doublet). A similar isotopic perturbation with CH_3OD has been described for $[IrH(\eta^1\text{-SpyH})(\eta^2\text{-Spy})(PPh_3)_2](BF_4)$ (**4**) [3].

2.3. Formation of $[IrH_2(\eta^1\text{-SpyH})_2(PPh_3)_2](BF_4)$ (2)

One of the triphenylphosphine ligands in $[IrH_2(SpyH)(PPh_3)_3](BF_4)$ (**1**) is replaced by another pyridine-2-thione ligand at r.t. over a period of one week. Thus, the product is a bis(triphenylphosphine) complex containing two SpyH proton donor groups. This is formulated as $[IrH_2(\eta^1\text{-SpyH})_2(PR_3)_2](BF_4)$ (**2**) (R = Ph) which is the triphenylphosphine analog to **5** (R = Cy) (Fig. 1). However, **2** is a difficult complex to isolate because it undergoes a further reaction to eliminate a dihydrogen molecule (Scheme 1).

Based on the following NMR observations, the structure of the species formed in this H_2 elimination reaction is proposed to be *trans*-$[IrH(\eta^1\text{-SpyH})(\eta^2\text{-Spy})(PPh_3)_2](BF_4)$ (**4′**) which is the *trans*-isomer of **4** that contains both chelating pyridinethiolate and monodentate pyridinethione ligands. The hydride resonance of **4′** at -16.68 ppm is a triplet ($J_{PH} = 12.21$ Hz) and the NH proton resonance at 11.91 ppm is a broad

singlet. These resonances are compared with those for **4** at −17.78 ppm as doublet of doublets for the hydride

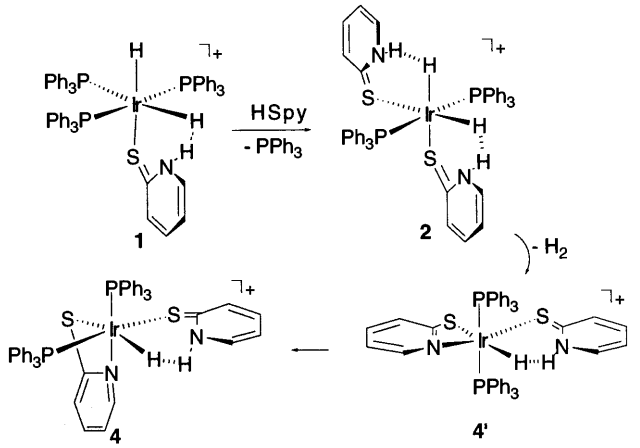

Scheme 1. Transformation of **1** to **4** via **2** and **4′**, the *trans* isomer of **4**.

Table 1
Comparison of the selected NMR [a] and T_{1min} calculations for **2** and **5**

	2	**5**
δ (NH)	11.70 (br s)	12.18 (br s)
T_{1min} (observed)	0.16 s (193 K)	0.18 s (233 K)
Total relaxation rate (s^{-1})	6.2	5.6
^{14}N contribution (s^{-1}) (1.0 Å)	1.4	1.4
Other contribution [b] (s^{-1}) (2.1 Å: one H of PPh_3)	1.4	
Sole contribution of H(Ir) (s^{-1})	3.4	3.1
T_1 (correct) (s)	0.28	0.23
d(HH) from T_1(NH) (Å)	1.74 ± 0.05	1.68 ± 0.05
δ(IrH) (t, $J = 15.3$ Hz)	−15.95	−18.28
T_{1min} (observed) (s)	0.20 (193 K)	0.17 (233 K)
Total relaxation rate (s^{-1})	5.0	5.9
Cis-hydride contribution (s^{-1}) [c]	0.9 (2.2 Å)	0.5 (2.4 Å)
PR_3 proton contributions (s^{-1}) [d]	1.5 (2.2 and 2.3 Å)	1.7 (2.2 and 2.2 Å)
Sole contribution of H(N) (s^{-1})	2.6	3.7
T_1 (correct) (s)	0.37	0.27
d(HH) from T_1(IrH) (Å)	1.82 ± 0.05	1.72 ± 0.05
Average d(HH) from T_1 (Å)	ca. 1.78	ca. 1.70
$^{31}P\{^1H\}$	9.4 (s)	8.21 (s)

[a] Chemical shifts in ppm, NMR measured in CD_2Cl_2 at 400 MHz. Relaxation rate contributions and d(HH) calculations done using the approach of Desrosiers et al. [13].

[b] Contribution from PCy_3 protons in **5** is not added because the position of the hydrides is uncertain.

[c] The typical distance between two *cis*-hydrides is assumed to be 2.4 Å in **5**.

[d] Two *trans*-PR_3 groups each with two CH protons near to the hydrides.

($J_{PH} = 14.3$ Hz) and 11.86 ppm as a broad singlet for the NH proton [3]. Although there are two possible *trans* isomers (i.e. the hydride *trans* to S or N of the chelate ring), Scheme 1 shows the one with the sulfur atom *trans* to the hydride, which would result from the stereospecific elimination of H_2 from **2**.

Complex **4′** is apparently an intermediate species observed by NMR spectroscopy in the transformation of **2** in $CDCl_3$ to the *cis*-product, **4** (Scheme 1). Complex **4′** has been also observed previously as an intermediate in the preparation of **4** from the reaction of the dihydride $IrH_2(\eta^2\text{-Spy})(PPh_3)_2$ with tetrafluoroboric acid in the presence of pyridine-2-thione [3].

2.4. Characterization of $[IrH_2(\eta^1\text{-SpyH})_2(PPh_3)_2](BF_4)$ (2)

Yellow crystals of **2** were obtained by fractional crystallization of the mixture of products from the reaction of **1** with one equivalent pyridine-2-thione by layering in $CHCl_3$ with ether. The NMR resonances for **2** are very similar to those for **5**, a PCy_3 analog (Table 1). In the proton NMR spectrum in CD_2Cl_2 the resonances for the NH protons and hydrides appear at 11.70 ppm as a broad singlet and −15.95 ppm as a triplet, respectively. The $^{31}P\{^1H\}$-NMR spectrum contains a singlet at 9.4 ppm. These results are consistent with the equivalence of ligand groups of two SpyH ligands, two hydrides and two phosphorus ligands. The short T_{1min} of 0.16 s for the NH protons and 0.20 s for the hydrides have been obtained for a solution of **2** in CD_2Cl_2 at 193 K, 400 MHz. These T_{1min} values and the relaxation rate contributions are compared with those for **5** in Table 1. The results suggest that the solution structure of **2** is very similar to that of **5**. The X-ray structure determination of **2** supports this conclusion (see Section 2.6).

2.5. Synthesis of $[IrH(CO)(SpyH)_2(PPh_3)_2](BF_4)_2$ (3)

Triphenylphosphine complexes containing carbonyls are often prepared from the reaction of commercially available transition metal chlorides with reactive organic carbonyl-containing compounds such as aldehydes or alcohols in the presence of a strong base [14]. In our attempt, a tris(triphenylphosphine)hydrido complex of Ir(III) was reacted with sodium hydroxide as a base and methanol as a carbonyl source, according to Eq.(3). A mixture of hydrido species consisting of a major (ca. 90%) and minor (ca. 10%) species was obtained. The hydride resonances for the major species in $CDCl_3$ appeared at −10.10 and −10.55 ppm as a triplet of doublets ($J_{PH} = 16.6$ Hz, $J_{HH} = 4.6$) and a triplet of triplets ($J_{PH} = 19.2$ Hz, $J_{HH} = 4.2$), respectively, with an intensity ratio of 2:1. In the $^{31}P\{^1H\}$-NMR spectrum there is a singlet at 16.29 ppm for the

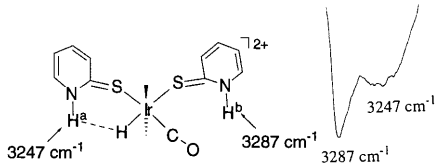

Fig. 4. Characteristic NH stretching wavenumbers for **3** (Nujol, KBr).

major species. The presence of a carbonyl ligand is confirmed by a strong ν(CO) band at 2077 cm^{-1}. These NMR and IR observations are consistent with a trihydrido carbonyl complex $IrH_3(CO)(PPh_3)_2$ [15]. The minor species was not identified.

$$IrHCl_2(PPh_3)_3 \xrightarrow[\text{(i) NaOH in THF, 20 h, RT, 20° under } H_2 \text{ (ii) MeOH / } H_2O]{\text{(i) (ii)}} IrH_3(CO)(PPh_3)_2 + \text{minor species} \quad (3)$$

When crude $IrH_3(CO)(PPh_3)_2$ was treated with HBF_4 in the presence of an excess of HSpy in $CDCl_3$, the suspension became clear yellow in about 10 min and a 1:1 mixture of two species was formed according to the ^{1}H-NMR spectrum. The products are proposed to be two dihydrido species $[IrH_2(CO)(\eta^1\text{-SpyH})(PPh_3)_2](BF_4)$ and $IrH_2(CO)(\eta^1\text{-Spy})(PPh_3)_2$ (Eq. (4)) based on the observation of one NH proton resonance (10.8 ppm) with two sets of hydride resonances of triplet of doublets: set 1: -7.28 ($J_{PH} = 17.5$, $J_{HH} = 4.56$ Hz) and -18.5 ppm ($J_{PH} = 14.04$, $J_{HH} = 4.68$ Hz) and set 2: -8.78 ($J_{PH} = 17.6$, $J_{HH} = 2.7$ Hz) and -13.9 ppm ($J_{PH} = 13.4$, $J_{HH} = 2.6$ Hz). The former is a monocationic species containing a monodentate SpyH ligand *cis* to one of the hydrides while the latter is a neutral species with a monodentate pyridinethiolate. These complexes, however, could not be isolated as they decomposed in less than 10 min to give several unidentifiable species.

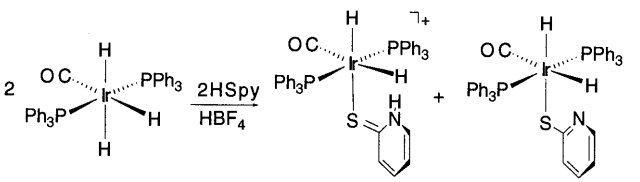

(4)

One of these species crystallized from chloroform solution by slow evaporation in the air over several weeks. The yellowish orange crystals were collected and analyzed by X-ray diffraction and infrared spectroscopy. They contain a dicationic monohydrido complex formulated as $[IrH(CO)(\eta^1\text{-SpyH})_2(PPh_3)_2](BF_4)_2$ (**3**) with two monodentate SpyH ligands, one of which is *cis* to the hydride and the other, *cis* to the carbonyl.

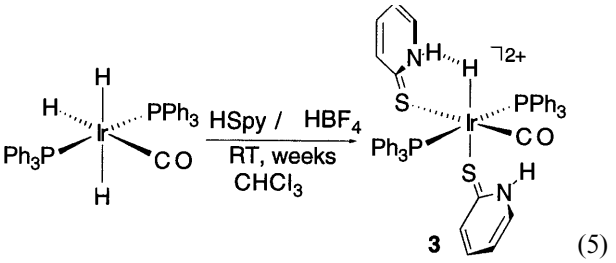

(5)

The IR spectrum of **3** in Nujol provides evidence for a carbonyl ligand and two types of NH units in the SpyH ligands. There is a strong band at 2044 cm^{-1} for the carbonyl ligand. There are two NH stretching frequencies at 3287 (sharp) and 3247 cm^{-1} (very broad) (Fig. 4). The NH^a···HIr interaction is probably responsible for the broadening of the peak at lower wavenumber. The NH^a stretching frequency of 3247 cm^{-1} in **3** is a little lower than that of non-hydrogen bonding SpyH at 3376 cm^{-1} [16]. The $\Delta\nu$ value of 129 cm^{-1} indicates that the NH^a···HIr interaction in **3** is relatively weak. Comparisons with other complexes will make this clearer in discussion further on. Another band at 3287 cm^{-1} is due to the NH^b unit which is not involved in proton–hydride bonding. The $\Delta\nu$ value of this band in comparison with ν(NH) of non hydrogen bonding SpyH is 89 cm^{-1}. This difference can be attributed to the perturbation in ν(NH) caused by the coordination of the ligand. However, it is difficult to confirm this since there is a very weak N–H···F hydrogen bond involving one of the BF_4^- counterions revealed by X-ray analysis (see later). For comparison purposes, however, both the ν(NH) of non hydrogen bonding free SpyH at 3376 cm^{-1} and the NH^b stretching frequency of 3287 cm^{-1} in **3** are arbitrarily used as references to calculate the difference ($\Delta\nu$) and to estimate an approximate bond energy using Iogansen's equation [17].

2.6. X-ray structural analyses for 1, 2 and 3

The summary of crystal data parameters is found in Table 2. Selected bond distances and angles for **1**, **2** and **3** are shown in Table 3. The ORTEP diagrams of the cations for **1**, **2** and **3** are shown in Figs. 5, 6 and 8, respectively.

Complex **1** is a cationic octahedral complex with three triphenylphosphine ligands, a monodentate pyridinethione ligand and two hydrides *trans* to a phosphine and a sulfur atom (Fig. 5). It has a mirror plane in the equatorial plane through atoms of the pyridinethione, the two hydrides and a phosphorus and one of its phenyl rings. Therefore half of the total atoms are assigned by symmetry relationship. The two hydrogens on the two nitrogens and the two *cis*-hydrides are well-defined in an electron difference map. One of the hydrides located at 1.81(8) Å from the iridium atom is in proximity to the NH proton at a

Table 2
Summary of crystal data, details of intensity collection, and least-squares refinement parameters for complexes **1**, **2** and **3**

Complex	**1**	**2**	**3**
Empirical formula	$C_{61}H_{54}BCl_6F_4IrNP_3S$	$C_{56.50}H_{54}BF_4IrN_2P_2S_2$	$C_{48}H_{43}B_2Cl_2F_8IrN_2OP_2S_2$
Crystal size (mm)	$0.42\times0.38\times0.44$	$0.63\times4.5\times3.1$	$0.10\times0.10\times0.10$
Formula weight	1417.73	1166.09	1226.63
Crystal class	Monoclinic	Monoclinic	Monoclinic
Space group	$P2_1/m$	$C2/c$	$P2_1/c$
Unit cell dimensions			
a (Å)	10.570(2)	37.528(4)	18.5325(1)
b (Å)	22.964(5)	15.280(2)	15.3441(2)
c (Å)	12.751(2)	23.387(3)	18.4464(2)
β (°)	102.199(12)	125.046(7)	94.221(1)
V (Å^3)	3025.3(10)	10979(2)	5231.27(9)
Z	2	8	4
D_{calc} (mg m^{-3})	1.556	1.411	1.557
μ(Mo–K$_\alpha$) mm^{-1}	2.638	2.617	2.861
F(000)	1416	4696	2432
T (K)	173(2)	213(2)	296(2)
Reflections collected	7034	11 983	40 443
Independent reflections	6686 ($R_{int}=0.0696$)	11 790 ($R_{int}=0.0465$)	9104 ($R_{int}=0.0443$)
Refinement method	Full-matrix least-squares on F^2	Full-matrix least-squares on F^2	Full-matrix least-squares on F^2
Data/restraints/parameters	6295/2/384	11782/2/531	9104/3/625
Goodness-of-fit on F^2	1.109	0.911	1.079
R_1 [$I>2\sigma(I)$]	0.0594	0.0461	0.0392
wR_2 (all data)	0.1677	0.1307	0.1099
Largest difference. peak and hole (e Å^{-3})	1.663 and −1.537	1.202 and −0.787	1.013 and −0.725

distance of about 2.1 Å. The two hydrides cause a lengthening of the *trans* M–L distances: Ir–S1 {2.469(3) Å} and Ir–P2 {2.414(3) Å}. Other structural features are compared with related structures later in this discussion.

Complex **2** is a structural analog to **5**. It is a monocationic iridium (III) complex containing two *trans* triphenylphosphine ligands and two monodentate pyridinethione ligands coordinated via sulfur atoms *trans* to two hydrides (Fig. 6). Two hydrides are located in the difference map at about 1.52 Å from the iridium atom. From the two elongated Ir–S distances {2.438(2), 2.447(2) Å}, the *trans* influence of the hydrides is evident. The NH···HIr distances are found to be 2.0–2.2 Å: a shorter distance (ca. 2.0 Å) in the H(2B)···H(2Ir) unit and a longer distance (ca. 2.2 Å) in the H(1A)···H(1Ir) unit.

The fluorines of the counterion BF_4^- of **2** are also weakly associated by hydrogen bonding to the NH units at about 2.4 Å. Both the NH units are involved in such intermolecular NH···FBF_3 hydrogen bonds to make a polymeric chain (Fig. 7). Note that the counterion BF_4^- of the PCy_3 analog **5** is observed to be farther away from the two NH units of the SpyH rings. As noted earlier, BF_4^- in **4** has been observed to form a hydrogen bond with an NH unit of a coordinated pyridinethione with a d(F···H) of ca. 2.0 Å [3].

Complex **3** is a dicationic octahedral complex with an iridium(III) centre surrounded by two triphenylphos-

Table 3
Selected bond distances (Å) and angles (°) for **1**, **2**, and **3**

Bond length		*Bond angles*	
1			
Ir–S1	2.469(3)	P1–Ir–P2	99.10(5)
Ir–P2	2.414(3)	P1–Ir–S1	91.30(5)
Ir–P1	2.329(2)	P1–Ir–H1	80.54(6)
Ir–H1 (Ir–H2)	1.81(8)	P1–Ir–H2	88.6(7)
H1···H(N2)	2.1(2)	P2–Ir–S1	97.8(1)
2			
Ir–P1	2.316(2)	P1–Ir–P2	171.08(6)
Ir–P2	2.315(2)	P1–Ir–S1	89.38(6)
Ir–S1	2.438(2)	P1–Ir–S2	95.83(6)
Ir–S2	2.447(2)	P2–Ir–S1	98.68(6)
Ir–H1 (Ir–H2)	1.52	P2–Ir–S2	89.36(6)
H(1Ir)···H(1A)	2.24	S1–Ir–S2	79.98(5)
H(2Ir)···H(2B)	2.03		
3			
Ir–P2	2.388(1)	P1–Ir–P2	174.81(4)
Ir–P1	2.387(1)	P1–Ir–S1	85.42(4)
Ir–S1	2.409(1)	P1–Ir–S2	95.53(4)
Ir–S2	2.478(1)	P2–Ir–S1	92.62(4)
Ir–C77	1.919(7)	P2–Ir–S2	88.75(4)
C77–O77	1.136(7)	S1–Ir–S2	78.14(4)
Ir–H1	1.58(4)	S1–Ir–C77	171.5(2)
H1···N1	2.42	S2–Ir–C77	110.3(2)
H1···H1A(N1)	2.1	P1–Ir–C77	93.0(2)
		P2–Ir–C77	88.2(2)
		Ir–C77–O77	171.6(6)

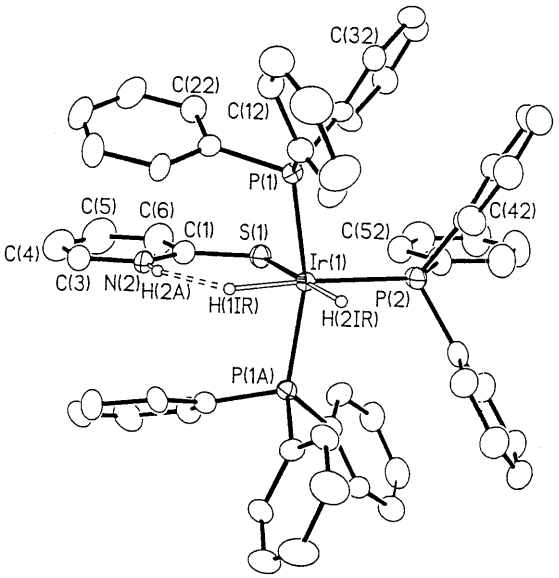

Fig. 5. ORTEP diagram of the cation of $[IrH_2(\eta^1\text{-SpyH})(PPh_3)_3](BF_4)$ (**1**) at 173 K.

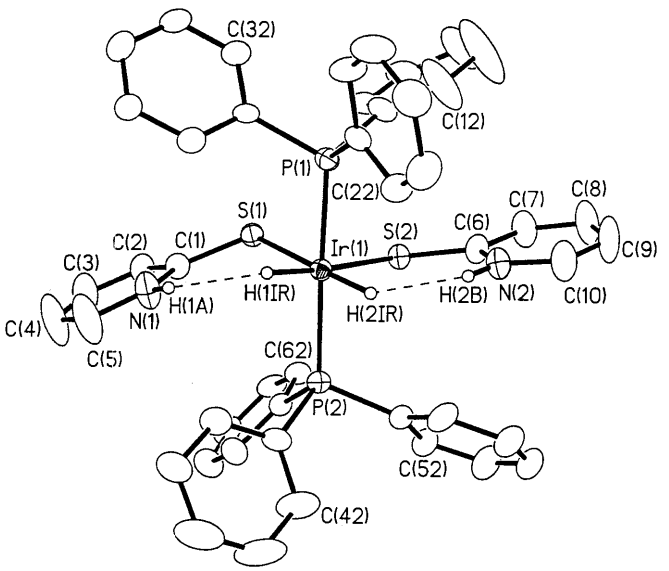

Fig. 6. ORTEP diagram of the cation of $[IrH_2(\eta^1\text{-SpyH})_2(PPh_3)_2](BF_4)$ (**2**) (213 K).

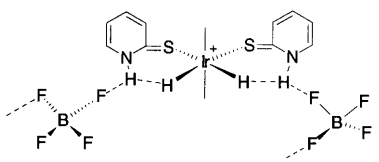

Fig. 7. Structure of **2** showing a hydrogen bonded polymeric chain with BF_4^- counterions.

phine ligands and two SpyH ligands cis to a hydride and a carbonyl ligand. The ORTEP diagram for **3** is shown in Fig. 8. Due to the presence of the *trans*-hydride, the Ir–S2 distance is longer {2.478(1) Å} than that for Ir–S1 {2.409(1) Å}. The hydride was located at 1.58(4) Å from the iridium atom. This places the hydride within about 2.1 Å of the NH proton of the *cis* SpyH ligand (IrH···N1 distance is about 2.62 Å). The SpyH ligand *cis* to the hydride is approximately in the equatorial coordination plane with a dihedral angle of 16.9° about the C6–S1 bond with respect to the plane consisting of Ir, H1, S1, S2, and C77. The pyridine unit of the other SpyH ligand *cis* to CO is much farther away from the coordination plane. The dihedral angle of this ring with respect to the plane is about 31.8° (Fig. 9). The *cis* S1–Ir–S2 angle {78.14(5)°} in **3** is not much different from those {80.88(6), 79.13(4)°} for **5** and **2**, respectively. Unusually wide angles of 128.3(5)° for S1–C6–N1 and 126.4(4)° for S2–C16–N11 are found. These are shown in Fig. 9 and compared with others in Table 4.

Similar to complex **2**, **3** appears to have a weak F···H–N hydrogen bond between one of the BF_4^- counterions and one of the SpyH ligands. The NH···F distance in the (N11)H···F2(B) unit is roughly 2.6 Å which is slightly less than the sum of the van der Waals radii of the two atoms in contact (H, 1.2 and F, 1.47 Å).

2.7. Comparison of the solid state structures containing SpyH···HIr bonds

The angles and the bond distances around the coordinated SpyH ligands of six iridium(III) complexes characterized by X-ray analyses are listed in Table 4. All are

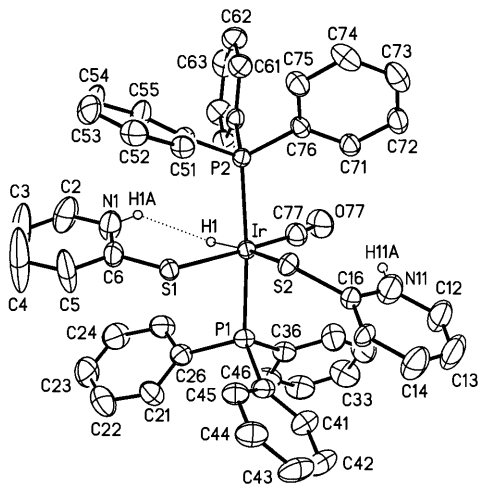

Fig. 8. ORTEP diagram of the cation of $[IrH(CO)(\eta^1\text{-SpyH})_2(PPh_3)_2]\text{-}(BF_4)_2$ (**3**) at 296 K.

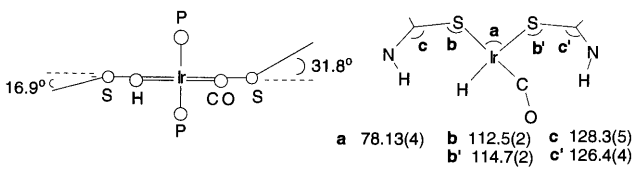

Fig. 9. Angles in the SpyH ligands of **3**.

Table 4
Selected angles and bond distances around the SpyH ligands [a]

	1	2	3	4	5	6
a	117.4(4)	113.7(2)	112.4(2)	114.4(3)	111.7(3)	113.1(2)
b	122.7(9)	122.3(5)	128.3(5)	122.7(6)	120.4(6)	122.5(5)
c [b]	$2.469(3)_{(H)}$	$2.438(2)_{(H)}$	$2.409(1)_{(CO)}$	$2.394(2)_{(P)}$	$2.451(2)_{(H)}$	$2.355(2)_{(S)}$
d	1.70(1)	1.702(6)	1.698(6)	1.730(8)	1.707(7)	1.714(6)
e	3.72(1)	3.62(1)	3.67(1)	3.61(1)	3.49(1)	3.52(1)
a		113.1(2)	114.6(2) [c]		113.5(2)	112.2(3)
b		121.8(5)	126.4(4) [c]		121.4(5)	123.4(6)
c [b]		$2.447(2)_{(H)}$	$2.478(1)_{(H)}$ [c]		$2.434(2)_{(H)}$	$2.351(2)_{(S)}$
d		1.696(7)	1.721(5) [c]		1.718(8)	1.705(8)
e		3.56(1)	3.91(1) [c]		3.55(1)	3.50(1)

[a] Angles *a*, *b* in degrees and distances *c*, *d* in Å. See Fig. 10 for the definition of these angles. Data are listed for two such ligands in **5**, **6**, **2**, and **3**.

[b] Atoms in brackets are *trans* atoms. Complexes **6** and **4** also have Ir–S distances (*trans* to hydride) in the chelating Spy ligand of 2.486(2) and 2.535(2) Å, respectively.

[c] Ligand *cis* to CO that is not involved in proton–hydride bonding.

cationic species containing one or two SpyH ligands. These include two of the PCy_3 complexes (**5**, **6**) and four of the PPh_3 complexes (**1**–**4**) (Fig. 1). The angles, Ir–S–C and S–C–N are labeled as **a** and **b**, respectively, and the distances, Ir–S and S–C as **c** and **d**, respectively. The dimensions of the pyridine rings were not found to vary significantly but are consistent with pyridinethione-like character.

The sulfur angles **a** of monodentate SpyH ligands are in the range of 111 to 114° with an exception of 117.4(4)° for **1**. The carbon angles **b** in the range of 120 to 123° are similar to that {120.5(1)°} for free pyridinethione except for **3** {126.4(4) and 128.3(5)°}. One can expect that, the smaller the angles **a** and **b** in the plane of the Ir–H, the closer the NH unit can approach to the iridium hydride. The larger angles **a** or **b** in **1** and **3** are consistent with the longer NH···HIr distance.

The N···Ir distances **e** which are more reliable than the H···H distances may be a useful indicator of the latter distances. The distances range from 3.49 to 3.61 Å with the exceptions of complexes **1** (3.72 Å) and **3** (3.67 and 3.91 Å). The longer N···Ir distance of 3.91 Å is for the nitrogen on the non-interacting SpyH ring *cis* to the carbonyl ligand in **3**. In comparison of N···Ir distances {3.49(1), 3.55(1) Å} for **5** with those {3.62(1), 3.56(1) Å} for **2**, a slightly longer distance of ca. 0.13 Å is found for one of the SpyH rings in **2**.

In the structural series in Table 4, many of the sulfur atoms are *trans* to hydrides (X = H in Fig. 10) and the S–Ir distances are subject to their *trans* influence. The S–Ir distances in the influence are 2.44–2.54 Å, longer than the normal S–Ir distances of 2.35–2.40 Å. However these variations in distance do not correlate with the N···Ir distances **e**. Shorter S–C distance **d** resulting from the SpyH ring having pyridinethione rather than protonated pyridinethiolate character (Fig. 11) do not apparently result in shorter N···Ir distances **e**.

The S–C distances **d** are found in the range from 1.696 to 1.730 Å which are comparable to that {1.698(2) Å} for the free pyridinethione dimer [18]. These are slightly shorter than those {1.724(7) and 1.741(7) Å} for the chelating η^2-pyridinethiolate ligands in **6** and **4**, respectively.

Table 5 shows a comparison of the selected angles and distances in the Ir–H···H–N units. The range of Ir–H···H(N) angles **A** (Fig. 12) is roughly 107–125° and the range of (Ir)H···H–N angles **B** is 135–156°. It should be noted that the NH is not directed toward the middle of the M–H bond as it is in the structure of the $ReH_5(PPh_3)_3$indole as determined by single crystal neutron diffraction [19]. The H···H distances are roughly in the range from 1.9 to 2.2 Å. The shortest H···H distance of 1.9 Å is in complex **6** which has the shortest Ir···N distances among the complexes given in Table 5.

Complexes **1** and **2** are related by replacing a PPh_3 ligand with a proton–hydride bonded SpyH ligand (Fig. 1). In both complexes, the SpyH ligands have pyridinethione character and the Ir–S distances show evidence of a *trans* hydride influence. The N···Ir distances in **2** are significantly shorter than that in **1** (Table

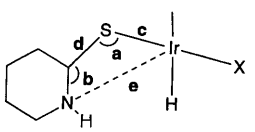

Fig. 10. Definition of the distances and angles listed in Table 4.

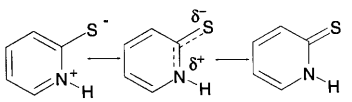

Fig. 11. Three resonance structures of protonated pyridinethiolate and pyridinethione.

Table 5
Comparison of the selected angles and distances in Ir–H···H–N units [a]

Complex	$d_{(Ir\cdots N)}$ (Å)	$d_{(Ir-H)}$ (Å)	$d_{(N-H)}$ (Å)	d_{HH} (Å)	A (°)	B (°)	Interacting unit
6	3.50(1) 3.52(1)	1.61(3)	0.78(7) 0.70(6)	1.9 1.9	108 119	144 145	N(32)–H(32A)···H–Ir N(22)–H(22A)···H–Ir
4	3.61(1)	1.7(1)	0.94(8)	2.1(1)	112	142	N(2)–H(2A)···H–Ir
1	3.72(1)	1.81(8)	0.88	2.1(2)	107	156	N(2)–H(2A)···H–Ir
2	3.56(1) 3.62(1)	1.52	0.87 0.87	2.0 2.2	109 114	149 154	N(1)–H(1A)···H(1)–Ir N(2)–H(2B)···H(2)–Ir
3	3.67(1)	1.58(4)	0.86	2.1	125	135	N(1)–H(1)···H–Ir

[a] See Fig. 12 for the definition of angles A and B.

4). The $(PPh_3)_3$ donor set in **1** makes the hydride less hydridic and therefore a weaker hydrogen-bond acceptor than the $(PPh_3)_2$(SpyH) donor set in **2**. Both the larger Ir–S–C angle **a** of 117.4(4)° and the longer N···Ir distance (ca. 3.72 Å) in **1** reflect this weaker NH···HIr interaction. The Ir–S–C bond angle **a** is flexible and can close down from 117 in **1** to 113° in **2** while all the other angles in the IrSCNH···H ring remain constant. The flexibility of the Ir–S–C angle is due in part to the ease of change of C–S bond character from thione to thiolate (Fig. 11).

Complexes **2** and **3** are related by replacing a hydride ligand with a carbonyl ligand (Fig. 1). There are substantial differences at the angle **b** which reflect the significant differences in the N···Ir distances between **2** and **3**. The large angles **b** {126.4(4), 128.3(5)°} in **3** are very unusual for an sp^2 carbon. It is not clear why the carbon angles **b** in **3** are out of the range of all others of the series in Table 4.

Based on the N···Ir distances, the relative strength of the proton hydride bonds may be roughly arranged as shown in the first row of Table 6. Table 6 also lists the donor ligands that may affect the strength of proton hydride bonds. The stronger proton hydride bonds occur when the co-donor ligands are the more basic PCy_3 ligands, while weaker proton hydride bonds occur when they are the less basic PPh_3. The hydricity of the hydride that is two bonds away from the substituent change will be affected more by this change than the acidity of the N–H group that is remote from this change in electronics. Furthermore, in the series, the weakest bonds are observed when a complex has three PPh_3 or two PPh_3 with a CO. Clearly an S_2P_2 donor set makes the hydride a better acceptor than the SP_3 donor set.

2.8. Comparison of spectroscopic features of proton hydride bonds

Table 7 summarizes some important NMR and IR features for the proton hydride bonds in the SpyH complexes prepared in this study. Two PCy_3 complexes **5** and **6** and three PPh_3 complexes **1**, **2** and **4** are examined by T_{1min} measurements. The H···H distances calculated from T_{1min} are in the range from 1.7 to 1.8 Å for the PCy_3 and PPh_3 complexes. Table 7 also includes the differences of the NH stretching frequencies in comparison with that of non-hydrogen bonding SpyH as well as with that of the SpyH unit (NH^b) in **3** that is weakly hydrogen-bonded to the BF_4^- counterion. The differences ($\Delta\nu$) vary from 265 to 129 cm^{-1} in comparison with the former and from 176 to 40 cm^{-1} in comparison with the latter. If we apply Iogansen's equation to estimate approximate energy changes using the $\Delta\nu$ values, the strength of the proton–hydride bond can be from 5 to 3 kcal mol^{-1} with respect to the ν(NH) of free SpyH and 4–1 kcal mol^{-1} with respect to the $\nu(NH^b)$ of complex **3**. These results again indicate that proton–hydride bonds are stronger in complexes with PCy_3 than with PPh_3 donor ligands.

Fig. 13 shows the relative strength of proton hydride bonds and N–H covalent bonds on an IR scale in comparison with those between the two extreme cases (pyridinethione dimer and dilute SpyH). It shows that the N–H···H–Ir proton hydride bonds in PCy_3 and PPh_3 complexes are attractive. The proton hydride bonds in PCy_3 complexes are slightly stronger than those in PPh_3 complexes, but weaker than the conventional N–H···S hydrogen bond in the pyridinethione dimer.

3. Conclusions

Three new iridium hydride complexes containing proton–hydride bonds are identified in this work. The NH···HIr distances in these complexes are ca. 2.0–2.1 Å by X-ray diffraction and 1.7–1.8 Å by ^{1}H-NMR. The best indicators of H···H bond strength are the $\Delta\nu$

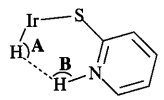

Fig. 12. Definition of the angles listed in Table 5.

Table 6
Comparison of the N···Ir distances versus co-donor ligands

Complexes [a]	**5** ≈	**6** >	**2** >	**4** >	**3** >	**1**
N···Ir (Å)	3.49(1) 3.55(1)	3.50(1) 3.52(1)	3.56(1) 3.62(1)	3.61(1)	3.67(1)	3.72(1)
Trans to H	S	S	S	S	S	PPh_3
Cis to H	PCy_3	PCy_3	PPh_3	PPh_3	PPh_3	PPh_3
Cis to H	PCy_3	S	PPh_3	PPh_3	PPh_3	PPh_3
Cis to H	H	N	H	N	CO	H
Cis to H	S	S	S	S	S	S

[a] N···Ir distances are increasing in the order from complex **5** to complex **1**

Table 7
T_{1min} from ^{1}H-NMR and IR bands for IrH and NH groups [a,b]

Compound	T_{1min} (IrH)	T_{1min} (NH)	*d* (H···H) (Å) [c]		*d* (Ir···N)
1	0.18 0.23 [d]	0.22	1.8 ± 0.05		3.72(1)
2	0.20	0.16	1.8 ± 0.05		3.56(1) 3.62(1)
4	0.27	0.24	1.8 ± 0.05		3.61(1)
5	0.17	0.18	1.7 ± 0.05		3.49(1) 3.55(1)
6	0.17	0.22	1.7 ± 0.05		3.50(1) 3.52(1)
	v(IrH) (cm^{-1})	*v*(NH) (cm^{-1})	Δv (cm^{-1}) [e]	Δv (cm^{-1}) [f]	d(Ir···N)
SpyH [g]		3376 [h]			
1	2063, 2197	3225	151	62	3.72(1)
3	2180, 2216	3247 3287 [i]	129 89	40 0	3.67(1) 3.91(1)
4	2214	3236	140	51	3.61(1)
5	2137, 2120	3111 3184	265 192	176 103	3.49(1) 3.55(1)
6	2193	3124	252	163	3.50(1) 3.52(1)
SpyH (dimer)		2900	476		

[a] Proton NMR and T_{1min} (s) measured in CD_2Cl_2 at 400 MHz.
[b] IR spectra measured in Nujol using KBr unless otherwise stated.
[c] H···H distances are estimated as discussed earlier.
[d] Values are for the hydride not associated with the proton–hydride bond.
[e] Reduction of *v* from *v*(NH) of free SpyH of 3376 cm^{-1}.
[f] Reduction of *v* from *v*(NH^b) at 3287 cm^{-1} in **3**.
[g] Dilute solution of SpyH in CCl_4, regarded as non-hydrogen bonding species [16].
[h] *v*(NH) of free SpyH.
[i] *v*(NH^b) not involved in proton–hydride bonding.

values from IR and the N···Ir distance from the X-ray structures. The new dihydride $[IrH_2(\eta^1\text{-SpyH})(PPh_3)_3](BF_4)$ **1** has the weakest IrH···HN interaction of six comparable complexes because it is the most congested and it has less basic ligands. Complex **1** provides a route to $[IrH_2(\eta^1\text{-SpyH})_2(PR_3)_2](BF_4)$ (**2**) (R = Ph) which is usefully compared with the tricyclohexylphosphine analog (**5**) (R = Cy). The less basic PPh_3 ligands of **2** result in less hydridic hydrides and therefore weaker IrH···HN bonds than in **5** that has the strongest such bonds of the series. Complex **2** slowly eliminates a dihydrogen molecule to form the known complex $[IrH(\eta^1\text{-SpyH})(\eta^2\text{-Spy})(PPh_3)_2](BF_4)$ (**4**) under mild conditions. The complex $[IrH(CO)(\eta^1\text{-SpyH})_2(PPh_3)_2](BF_4)_2$ (**3**) contains both a proton–hydride bonded SpyH ligand and a SpyH ligand that is weakly hydrogen-bonded to a BF_4^-. Like **1**, the NH···HIr bond in **3** is weak because of the presence of the electron-withdrawing carbonyl ligand.

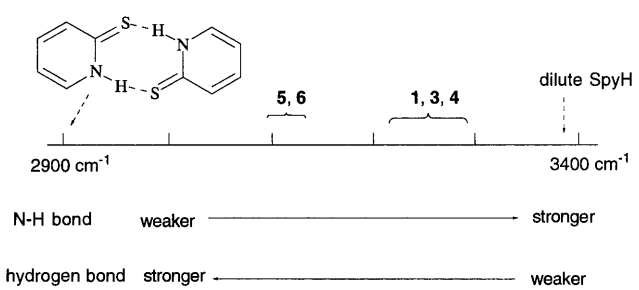

Fig. 13. Comparison of the NH stretching frequencies of coordinated and free SpyH.

4. Experimental

4.1. General procedures

All preparations were carried out under an atmosphere of dry argon using conventional Schlenk techniques. All the solvents were distilled under argon over appropriate drying agents prior to use. Tetrahydrofuran (THF) and diethyl ether (Et_2O) were dried over and distilled from sodium benzophenone ketyl. Methanol was dried over sodium methoxide. Dichloromethane and chloroform were distilled from calcium hydride. Deuterated solvents were dried over Linde type 4 Å molecular sieves and degassed prior to use. Distilled water was degassed prior to use. Triphenylphosphine, pyridine-2-thione, sodium hydroxide and an 85% solution of HBF_4Et_2O complex were purchased from Aldrich Chemical Company Inc. Iridium trichloride hydrate was obtained from Johnson–Matthey Co. Sodium ethoxide was generated in the reaction of sodium metal with water-free ethanol under argon and dried to a white powder before use.

NMR spectra were obtained on a Unity-400, operating at 400.00 MHz for ^1H, 161.98 MHz for ^{31}P, or on a Gemini-300 operating at 300.00 MHz for ^1H, 121.45 MHz for ^{31}P. All ^{31}P-NMR spectra were obtained with proton decoupling unless otherwise stated. ^{31}P-NMR chemical shifts were measured relative to H_3PO_4 as internal reference. ^1H-NMR chemical shifts were measured relative to deuterated solvent peaks or tetramethylsilane. Variable temperature T_1 measurements were made at 400 MHz using the inversion recovery method. Microanalysis was performed by Guelph Chemical Laboratories Ltd., Ontario.

4.2. Crystallographic structural determination

Complexes **1**, **2** and **3** were crystallized by the slow evaporation of a chloroform solution at r.t. A single crystal for **1**, **2** and **3** suitable for X-ray analysis was mounted with epoxy glue and analyzed at 173 (**1**), 213 (**2**) and 296 K (**3**). The crystalline system for **1** was found to be monoclinic with space group $P2_1/m$. The unit cell dimensions of the crystal are $a = 10.570(2)$, $b = 22.964(5)$ Å with $\beta = 102.199(12)°$, and $c = 12.751(2)$ Å. The crystal for **2** has the monoclinic space group $C2/c$ with unit cell $a = 37.528(4)$, $b = 15.280(2)$ Å with $\beta = 125.046(7)°$, and $c = 23.387(3)$ Å. Intensity data for **1** and **2** were collected on a Siemens P4 diffractometer, using graphite monochromated Mo–K_α radiation ($\lambda = 0.71073$ Å). The ω scan technique was applied with variable scan speeds. Intensities of three standards measured for each compound every 97 reflections showed no decay. Data were corrected for Lorentz, and polarization effects and for absorption. The Ir atom position in the structure of **1** and **2** was solved by the Patterson method and other non-hydrogen atoms were located by successive difference Fourier syntheses. Non-hydrogen atoms were refined anisotropically by full-matrix least-squares on F^2. Hydrogen atoms were positioned on geometric grounds (C–H 0.96 Å). All calculations were done and diagrams created using SHELXTL PC on a Pentium-75 personal computer.

The crystal for **3** belongs to monoclinic space group $P2_1/c$ with unit cell $a = 18.5325(1)$, $b = 15.3441(2)$ Å with $\beta = 94.221(1)°$, and $c = 18.4464(2)$ Å. The structure was solved by direct methods, completed by subsequent Fourier synthesis, and refined by full-matrix least-squares procedures. The two counterions, and chloroform solvent molecule were located. All boron–fluorine interatomic separations were restrained to be equal. All other non-hydrogen atoms were refined with anisotropic displacement coefficients. The hydride H1 was located from a difference map and refined with a riding model.

Crystal data, data collection, and least squares parameters are listed in Table 2 and selected bond distances and angles are in Table 3. Views of cations of complexes **1**, **2** and **3** including the crystallographic labeling scheme are shown in Figs. 5, 6 and 8, respectively.

4.3. Preparation of $[IrH_2(\eta^1\text{-}SpyH)(PPh_3)_3](BF_4)$ (**1**)

4.3.1. Method 1

4.3.1.1. Reaction of fac-$IrH_3(PPh_3)_3$ with HSpy and HBF_4. *fac*-$IrH_3(PPh_3)_3$ (1 g, 1.0 mmol) and HSpy (113 mg, 1.0 mmol) were suspended in $CHCl_3$ (15 ml) in a Schlenk flask under argon. To this was added excess HBF_4 (500 μl in ether solution). The solution became clear yellow in a few min. After 10 min the clear solution was filtered through Celite. The solvent was then removed in vacuo. The resulting residue was washed with ether several times (10 ml × 3) to give a bright yellow powder. This was further dried in vacuo. Yield: 1.1 g, 91%.

4.3.2. Method 2

4.3.2.1. Reaction of $IrH_3(PPh_3)_3$ (fac- and mer- mixture) with HSpy and HBF_4. A mixture of *fac*- and *mer*-$IrH_3(PPh_3)_3$ (1 g, 1.0 mmol) and HSpy (113 mg, 1.0 mmol) were suspended in CH_2Cl_2 (15 ml) under argon. To this was added excess HBF_4 (500 μl in ether solution). The work up was similar to that of Section 4.3.1 with similar yield: Anal. Calc. for $C_{59}H_{52}BF_4IrNP_3S\cdot CHCl_3$: C, 55.5; H, 4.12; N, 1.08. Found: C, 55.72; H, 4.35; N, 1.06%. NMR ($CDCl_3$, δ). $^{31}P\{^1H\}$: 2.23 (d, $J = 15.2$ Hz), −0.93 (t, $J = 15.6$ Hz); ^1H: −12.7 (dtd, $J^t_{PH} = 116$, $J^c_{PH} = 22$, $J_{HH} = 3.6$ Hz, 1H, Ir–*H*), −15.75 (qd, $J_{HH} = 3.6$, 1H, Ir–*H*), 6.4–7.8 {m, 49 H, overlap-

ping $P(C_6H_5)_3$ with $SC_5H_4NH^+$}, 10.9 {br s, 1H, ($SC_5H_4NH^+$)}. IR (KBr pellet): ν(Ir–H), 2063, 2197 cm^{-1}; ν(NH), 3225 cm^{-1}.

4.4. Formation of $[IrH_2(\eta^1\text{-SpyH})_2(PPh_3)_2](BF_4)$ (2)

$[IrH_2(\eta^1\text{-SpyH})(PPh_3)_3](BF_4)$ (**1**) (100 mg, 0.085 mmol) and HSpy (53 mg, 0.477 mmol) dissolved in $CHCl_3$ (6 ml) were added to a Schlenk flask fitted with a magnetic stirring bar under argon. This was stirred for over a week at r.t. The solution was monitored by $^{31}P\{^1H\}$-NMR. There was a major species with a resonance at 9.4 ppm (s) and a minor species at −9.97 ppm (s) in addition to unreacted **1**. The solution was further stirred for a second week and checked by $^{31}P\{^1H\}$-NMR; no more unreacted **1** was observed. All the volatiles were then removed in vacuo. To the residue was added ether (10 ml) to wash out excess HSpy and to give a light yellow powder. Three species were observed by $^{31}P\{^1H\}$-NMR: the major species was $[IrH_2(\eta^1\text{-SpyH})_2(PPh_3)_2](BF_4)$ (**2**) and the minor species are *trans*-$[IrH(\eta^1\text{-SpyH})(\eta^2\text{-Spy})(PPh_3)_2](BF_4)$ (**4′**) and *cis*-$[IrH(\eta^1\text{-SpyH})(\eta^2\text{-Spy})(PPh_3)_2](BF_4)$ (**4**). The intensities of the minor resonances grow over time as the intensity of the resonances for the major species decreases. The final spectrum is consistent with that for *cis*-$[IrH(\eta^1\text{-SpyH})(\eta^2\text{-Spy})(PPh_3)_2](BF_4)$ (**4**) [3]. Selected proton NMR resonances (δ): NH: 11.74 (br s, **2**); 11.91 (br s, **4′**); 11.86 (br s, **4**). IrH: −16.10 (t, $J_{PH} = 15.3$ Hz, **2**); −16.68 (t, $J_{PH} = 12.21$ Hz, **4′**); −17.78 (dd, $J_{PH} = 14.3$ Hz, **4**).

4.5. Preparation of crude $IrH_3(CO)(PPh_3)_2$

$IrHCl_2(PPh_3)_3$ [20] (500 mg, 0.476 mmol) was suspended in THF (25 ml) in a Schlenk flask fitted with a stirring bar under dihydrogen gas. To this was added ground sodium hydroxide (1 g, 0.025 mol). The suspension was stirred for about 20 h at r.t. followed by evaporation of the solvent. To the residue was added degassed water (ca. 20 ml). This was stirred for 10 min before filtration. The wet residue was stirred in methanol (ca. 20 ml) for 10 min. This was followed by a vacuum filtration and drying to obtain a pale grey yellow powder. This was washed with ether (2 × 10 ml) and dried in vacuo. Yield: 280 mg, 78% based on $IrH_3(CO)(PPh_3)_2$ [15]. NMR ($CDCl_3$, δ) for the major species. $^{31}P\{^1H\}$: 16.29 (s); ^1H: −10.10 (td, $J_{PH} = 16.62$ Hz, $J_{HH} = 4.6$ Hz, 2H, Ir–*H*), −10.55 (tt, $J_{PH} = 19.2$, $J_{HH} = 4.2$ Hz, 1H, Ir–*H*), 6.4–7.9 {m, 30H, $P(C_6H_5)_2$}. IR (KBr, Nujol): ν(CO), 2077 cm^{-1} (s). Selected NMR ($CDCl_3$, δ) for the minor species; $^{31}P\{^1H\}$: 8.25 (s); ^1H: −15.4 (t).

4.6. Crystallization of $[IrH(CO)(\eta^1\text{-SpyH})_2(PPh_3)_2](BF_4)_2$ (3)

In a Schlenk flask crude $IrH_3(CO)(PPh_3)_2$ (50 mg, 0.07 mmol) and HSpy (18 mg, 0.16 mol) were dissolved in $CHCl_3$ (2 ml). To this was added an excess of HBF_4 etherate and allowed to react for 10 min during which time gas evolution occurred and the solution became clear yellow. This was left for slow evaporation at r.t. in air for about a week resulting in some orange–yellow crystals deposited among a yellow powder. The crystals were collected and used for X-ray analysis and infrared studies. IR (KBr, Nujol): ν(CO), 2044 cm^{-1} (s); ν(IrH), 2180, 2216 cm^{-1} (m); ν(NH), 3247 (w, br), 3287 cm^{-1} (w).

5. Supplementary material

Crystallographic data (excluding structure factors) for the structures reported in this paper have been deposited with the Cambridge Crystallographic Data Centre, CCDC nos. 140155 (**1**), 140156 (**2**), 140093 (**3**). Copies of this information may be obtained free of charge from The Director, CCDC, 12 Union Road, Cambridge CB2 1EZ, UK (Fax: +44-1223-336033; e-mail: deposit@ccdc.cam.ac.uk or www: http://www.ccdc.cam.ac.uk).

Acknowledgements

NSERC Canada is thanked for an operating grant to RHM.

References

[1] A.J. Lough, S. Park, R. Ramachandran, R.H. Morris, J. Am. Chem. Soc. 116 (1994) 8356.
[2] S. Park, R. Ramachandran, A.J. Lough and R.H. Morris, J. Chem. Soc. Chem. Commun. (1994) 2201.
[3] S. Park, A.J. Lough, R.H. Morris, Inorg. Chem. 35 (1996) 3001.
[4] W. Xu, A.J. Lough, R.H. Morris, Inorg. Chem. 35 (1996) 1549.
[5] W. Xu, A.J. Lough, R.H. Morris, Can. J. Chem. 75 (1997) 475.
[6] K. Abdur-Rashid, D.G. Gusev, S.E. Landau, A.J. Lough, R.H. Morris, J. Am. Chem. Soc. 120 (1998) 11826.
[7] J.C. Lee, E. Peris, A.L. Rheingold, R.H. Crabtree, J. Am. Chem. Soc. 116 (1994) 11014.
[8] E. Peris, J.C. Lee, J.R. Rambo, O. Eisenstein, R.H. Crabtree, J. Am. Chem. Soc. 117 (1995) 3485.
[9] E. Peris, J. Wessel, B.P. Patel, R.H. Crabtree, J. Chem. Soc. Chem. Commun. (1995) 2175.
[10] R.C. Stevens, R. Bau, D. Milstein, O. Blum, T.F. Koetzle, J. Chem. Soc. Dalton Trans. (1990) 1429.
[11] R.H. Crabtree, P.E.M. Siegbahn, O. Eisenstein, A.L. Rheingold, Acc. Chem. Res. 29 (1996) 348.
[12] J. Chatt, R.S. Coffey, B.L. Shaw., J. Chem. Soc. (1965) 7391.

[13] P.J. Desrosiers, L. Cai, Z. Lin, R. Richards, J. Halpern, J. Am. Chem. Soc. 113 (1991) 4173.
[14] N. Ahmad, J.J. Levinson, S.D. Robinson, M.F. Uttley, Inorg. Synth. 15 (1974) 45.
[15] J.F. Harrod, W.J. Yorke, Inorg. Chem. 20 (1981) 1156.
[16] P. Mura, B.G. Olby, S.D. Robinson, J. Chem. Soc. Dalton Trans. (1985) 2101.
[17] E.S. Shubina, N.V. Belkova, L.M. Epstein, J. Organometal. Chem. 536 (1997) 17.
[18] U. Ohms, H. Guth, A. Kutoglu, C. Scheringer, Acta Cryst. B38 (1982) 831.
[19] J. Wessel, J.C. Lee, E. Peris, G.P.A. Yap, J.B. Fortin, J.S. Ricci, G. Sini, A. Albinati, T.F. Koetzle, O. Eisenstein, A.L. Rheingold, R.H. Crabtree, Angew. Chem. Int. Ed. 34 (1995) 2507.
[20] S. Brinkmann, R.H. Morris, R. Ramachandran, S. Park, Inorg. Synthesis 32 (1998) 303.